Chiral Recognition between α-Hydroxylesters: A Double-Resonance IR/UV Study of the Complexes of Methyl Mandelate with Methyl Glycolate and Methyl Lactate

Katia Le Barbu-Debus,*,† Michel Broquier,† Ahmed Mahjoub,† and Anne Zehnacker-Rentien†,‡

CNRS, Laboratoire de Photophysique Moléculaire, UPR3361, Orsay, France 91405, and University of Paris-Sud, Orsay, France 91405

Received: December 7, 2007; Revised Manuscript Received: May 21, 2008

Chiral recognition between α hydroxylesters has been studied in jet-cooled complexes of methyl mandelate with methyl lactate. The complex with nonchiral methyl glycolate has also been studied for the sake of comparison. The hydrogen-bond topology of the complexes has been interrogated by means of IR/UV double-resonance spectroscopy in the range of 3 μm. A theoretical approach has been conducted in conjunction with the experimental work to assist in the analysis of the spectra. Owing to the conformational flexibility of the subunits at play, emphasis has been put on the methodology used for the exploration of the potential-energy surface. The hydrogen-bond topology is very similar in the homo- and heterochiral complexes. It involves insertion of the hydroxyl group of methyl mandelate within the intramolecular hydrogen bond of methyl lactate or methyl glycolate, resulting in a five-membered ring. This contrasts with methyl lactate clusters previously studied by FTIR spectroscopy in a filet jet.[1]

I. Introduction

Chirality plays a major role in many fields of science, including most of the reactive processes related to life chemistry. Chiral recognition is the ability of a chiral molecule to differentiate between the two enantiomers of another chiral molecule by means of stereospecific interactions taking place in weakly bound complexes. To understand the nature of the forces responsible for this discrimination, we developed the study of weakly bound diastereomeric pairs at the molecular level.[2−10] A supersonic jet is used to stabilize and cool down to a few Kelvin weakly bound diastereomers isolated in the gas phase. The so-formed diastereomers are detected by LIF (laser-induced fluorescence) and IR/UV double-resonance spectroscopy. Complexation between the chromophore and a chiral partner induces a shift of the 0^0_0 transition relative to the bare molecule. Because of the stereospecificity of the chromophore−solvent interaction, this shift is different in the **RR** and **RS** pairs. In this way, specific spectroscopic signatures of the homo- and heterochiral complexes can be observed. Previous work in our group has consisted of studying complexation between monofunctional and bifunctional chiral molecules. We observed a dramatic chiral discrimination effect in both the size of the adduct formed and the nature of the hydrogen-bond network at play in the complex.[10−12] We will assess here the role of multiple hydrogen bonds by studying the influence of the bifunctionnal nature of the subunits in complexes built from two bifunctional molecules, namely, lactic acid esters.

Lactic acid esters have been studied extensively in jet-cooled conditions and show efficient cluster formation.[1,12−15] In particular, the methyl lactate dimer and its nonchiral analogue methyl glycolate have been studied by direct IR absorption in a filet jet.[1,13] The enantioselectivity of the hydrogen-bond pattern has been studied up to the tetramer. The influence of adding an aromatic ring to the same hydrogen-bond motif is studied by replacing the methyl lactate monomer by its aromatic analogue, methyl mandelate, described in this article. We report here the IR/UV double-resonance spectra of complexes between methyl mandelate and methyl lactate and methyl glycolate as well as an extensive theoretical exploration of the potential-energy surface describing their H-bond pattern. The methyl mandelate and methyl lactate molecules present two closely related structures. They are both derived from an ester of lactic acid and possess two functional groups (a hydroxyl group, OH and an ester group, RCOOR′). They present in their most stable form an intramolecular hydrogen bond from the OH to the CO groups. They only differ by the substituent on the carbon in the α position. The methyl mandelate molecule is tagged with a chromophore (the benzene ring with a $\pi \rightarrow \pi^*$ transition) which is absent in methyl lactate. This system allows us to address the role of the aromatic ring in the molecular interaction at play in α-hydroxyesters dimers.

Because of the complexity of the methylesters conformational landscape, emphasis is put on the methodology used for ensuring an exploration of the potential-energy surface of the complexes as exhaustive as possible. In particular, some assumptions in terms of binding and deformation energies are made in order to select the most pertinent configurations.

II. Experimental and Computational Methodology

1. Experimental Section. The sample vapors seeded in helium at a pressure of ∼2 atm were expanded into vacuum through a continuous or pulsed nozzle (General Valve). All compounds were purchased from Aldrich in their pure enantiomeric form and used as provided. The solid samples were placed in a porous cup (pores with 20 μm diameter) upstream of the conduit: they were heated in order to increase their vapor pressure.

The S_0-S_1 excitation spectra were obtained first by laser-induced fluorescence. The fluorescence signal from the sample is collected perpendicular to both the exciting light and the molecular beam by a two-lens collecting system and detected

* To whom correspondence should be addressed. E-mail: katia.le-barbu-debus@u-psud.fr.

† Laboratoire de Photophysique Moléculaire.

‡ University of Paris-Sud.

10.1021/jp711546p CCC: $40.75
Published on Web 09/09/2008

by a Hamamatsu R2059 photomultiplier. The output electrical signal of the PMT is averaged by an oscilloscope (Lecroy 9310) and finally processed through a personal computer. The first excited-state electronic spectroscopy is also characterized by one-color R2PI techniques. A Jordan time-of-flight spectrometer detects the formed ions by a two-photon process; the energy of the first photon is resonant with a vibronic state of the first excited state, and the second one allows the molecule to be ionized. The light source used for the S_0-S_1 spectroscopy consists of a frequency-doubled dye laser (Sirah, Spectra Physik, 0.03 cm^{-1} resolution) pumped by the third harmonic of a Nd:YAG (GCR 190, Spectra Physik).

The vibrational spectra in the region of 3 μm were obtained using the fluorescence-dip technique.[16−20] This pump−probe method rests on the use of two lasers; the UV laser (or probe) is tuned to an electronic transition of a given species, while the IR laser (pump) is scanned in the region of interest. When the pump is in resonance with a vibrational transition of the probed species, the resulting depletion of the ground state manifests itself as a dip in the probe-induced fluorescence. Besides its sensitivity, this method has the advantage of being isomer selective as it allows for recording separately the spectra of different species which absorb in the same energy range. The light sources used for the double-resonance experiments, in the range of the ν(OH) and ν(CH) stretch modes, are based on two OPO lasers synchronously pumped by a Nd^{3+}:YAG laser. This laser is pulsed at 20 Hz and has a particular temporal structure which consists of a long train of 50 micropulses of 12 ps separated by 10 ns. It is to be noticed that the absorption band of the $LiNBO_3$ crystal, located at 3494 cm^{-1} with a fwhm around 50 cm^{-1}, induces a dramatic diminution of the IR power in this range. However, depletion in this range of energy is still observed provided that the oscillator strengths of the observed vibrations were strong enough. This evidences the sensitivity of the method.

IR/UV double-resonance spectroscopy, associated with a R2PI detection, is used to record the vibrational spectrum of the bare methyl mandelate molecule in the fingerprint and C═O region (500−2000 cm^{-1}). In this case, the IR source is provided by the Free Electron Laser (FEL) of CLIO located at Orsay[21] and the UV source is a Euroscan visible OPO which is frequency doubled by use of a BBO crystal. Both the free electron laser and OPO have the same temporal shape as the OPO laser described previously; it is composed of macropulses at a repetition rate of 25 Hz, the macropulse being composed of 600 micropulses of 1 ps duration, separated from each other by 16 ns.

2. Theoretical Section. The equilibrium geometry and stabilization energies as well as the harmonic vibrational frequencies and transition intensities were calculated to provide a basis for comparison with the experimental spectra.

Exploration of the potential-energy surface of the complexes is divided into two different steps which have already been described elsewhere.[22] We first determine the minima of the potential-energy surface by means of a semiempirical method developed by Claverie[23] and extended by Brenner et al.[24] in which only the intermolecular coordinates were optimized. Second, we perform DFT calculations for a full optimization of the most stable isomers resulting from the semi empirical method.

The semi empirical method is based on the perturbation exchange theory and has been described elsewhere.[4,24] It rests on a description of the interaction energy as a sum of four terms (electrostatic, repulsion, polarization, and dispersion) which can be written analytically as a function of the intermolecular distances combined with a whole exploration of the potential-energy surface. The structure of the isolated molecules is first optimized at the MP2/6-31G(d,p) level of theory. The corresponding electronic distribution is then calculated at the MP2 level with the same basis set. This distribution is reduced to a multipolar−multicenter distribution by means of the procedure developed by Vigne-Maeder et al.[25] This allows us to evaluate the electrostatic term as a sum of multipolar interactions. The same multipolar−multicenter distribution, together with experimental atom and bond polarizabilities, is used for the polarization term, while a sum of atom−atom terms is used to describe the dispersion and repulsion contributions. The potential-energy surface is first explored by simulated annealing with the Metropolis algorithm.[26,27] Second, an energy optimization of all the minima found in the simulated annealing step is performed. At the end of this optimization, we get the different components of the interaction energy (electrostatic, polarization, repulsion, and dispersion) for each minimum of the potential-energy surface.

The 20 most stable complexes resulting from the previous step were fully optimized using DFT calculations. On the other hand, Borho et al. already calculated the structures of the methyl lactate dimers.[1,28] These authors identified cyclic structures, namely, C5 and C8. C5 means that a ring containing five heavy atoms is formed by including a hydroxyl in a preformed intramolecular hydrogen bond, which itself can be seen as a C4 four-membered ring. In the same way, C8 means that the intramolecular hydrogen bond of the two partners is disrupted to allow formation of a head to head double intermolecular hydrogen bond including eight heavy atoms. These structures have also been fully optimized by DFT calculations.

All calculations were carried out with the Gaussian 03 software package.[29] The complexes were locally optimized employing the B3LYP density functional with the standard 6-31G(d,p) basis set of Gaussian. The basis set superposition error (BSSE) is also calculated following the counterpoise method of Boys and Bernardi.[30] It turns out that the dissociation energy corrected by the BSSE deduced from the counterpoise method is underestimated. As suggested in previous work,[31] one-half of the BSSE value is used as a correction. Finally, harmonic frequencies were obtained at the same level of theory. The dissociation energies (DE) relative to the closest stable fragment given in the text include both total ZPE and 50% BSSE corrections. Deformation energies were also calculated as the energy difference between the optimized geometry and the geometry adopted in the complex by the entity under interest.

As DFT methods do not account for dispersion forces, which may be important in such systems,[10] optimization at the MP2/6-31G(d,p) level of theory of the most relevant structures is performed to see whether their relative binding energies were modified. The binding energies (BE) given in the text are the interaction energy De values obtained at the MP2/6-31G(d,p) level of theory (De_{mp2}) corrected by 50% of the BSSE calculated at the MP2/6-31G(d,p) ($BSSE_{mp2}$).

The size of the system precludes any frequency calculation at the MP2/6-31(d,p) level of theory: all simulated vibrational spectra were obtained at the B3LYP/6-31G(d,p) level of theory and corrected by a scaling factor of 0.96 in the ν(CH) and ν(OH) region.

III. Experimental Results

1. One-Bare Molecule Spectroscopy. The methyl mandelate excitation spectrum in the region of the 0^0_0 origin transition is

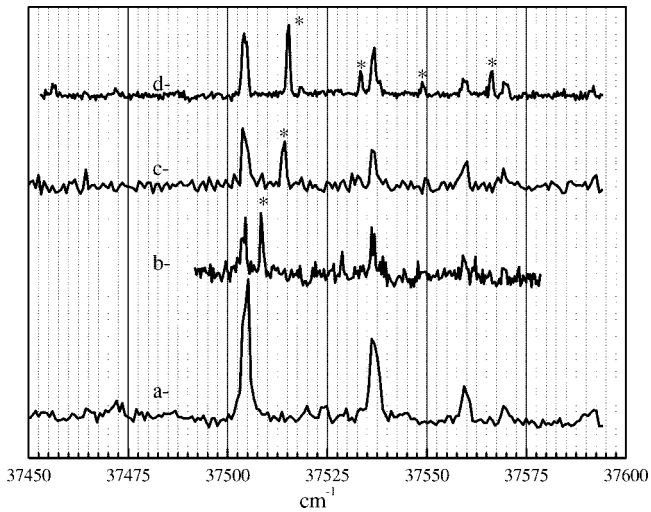

Figure 1. Laser-induced fluorescence excitation spectra (LIF) of jet-cooled (a) *R*-methyl mandelate bare molecule, (b) **RS** methyl mandelate/methyl lactate diastereoisomer, (c) **RR** methyl mandelate/methyl lactate diastereoisomer, and (d) methyl mandelate/methyl glycolate complex. Features indicated by an asterisk are due to complexation.

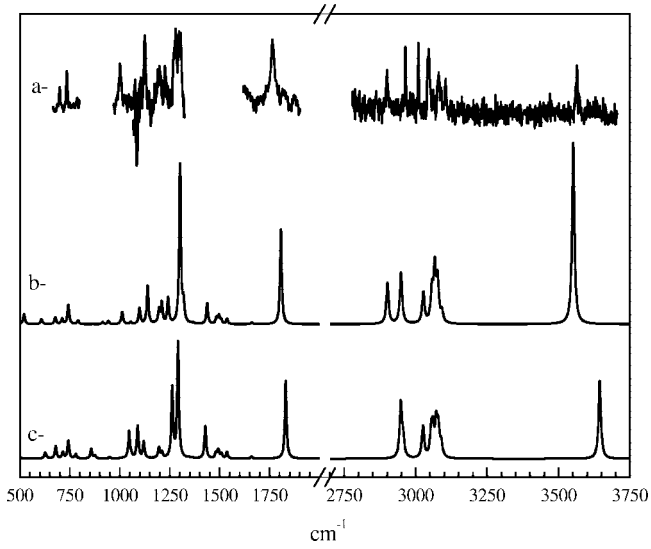

Figure 2. Experimental and theoretical IR spectra of methyl mandelate bare molecule: (a) experimental spectrum obtained with the OPO laser in the CH/OH stretch region and with the FEL of CLIO in the region below 1800 cm^{-1}, (b) calculated spectrum for the SsC conformer of methyl mandelate, and (c) calculated spectrum for the G′sk′C conformer of methyl mandelate.

presented in Figure 1a. The intense 0^0_0 transition located at 37 503 cm^{-1} (origin of energies) is followed by two bands of lower intensity at +31 and +55 cm^{-1}. These bands are due to the activity of vibrational modes of low frequencies (torsion of the substituent). The excitation spectra are identical for a racemic mixture or the pure enantiomers (R or S).

An IR/UV depletion spectrum by the R2PI method is recorded in the range of the ν(OH) and ν(CH) stretch vibrational frequencies. The probe is fixed on the origin transition at 37 503 cm^{-1} (Figure 2a). We observe in the region of the ν(OH) stretch mode a narrow band at 3565 cm^{-1}, at the same frequency as observed in the methyl lactate spectrum.[1] We can conclude from this result that the presence of a remote benzene ring does not modify the nature of the lactate intramolecular H bond. The ν(OH) stretch frequency is lower than that measured for an aliphatic alcohol, for example, at 3677 cm^{-1} for the anti conformer of ethanol[32] and comparable with other systems exhibiting an intramolecular hydrogen bond (aminoethanol[33] ν(OH) = 3569 cm^{-1}). This lowering reflects the presence of an intramolecular hydrogen bond between OH and C═O. In the range of the ν(CH) vibrations,[34] the spectrum can be separated in two regions, the aromatic ν(CH) stretch modes around 3045 cm^{-1} and the aliphatic ν(CH) stretch modes characterized by three bands at 2900, 2964, and 3009 cm^{-1}.

The same ν(OH) vibrational frequency has been measured by non resonant ionization-detected IR spectroscopy. In this experiment, the wavelength of the UV laser is set just below the first excited-state energy (55 cm^{-1} below the origin transition), so that no ion is observed without IR laser. The IR laser is then tuned. When it is resonant with a vibrational transition of jet-cooled methyl mandelate, the vibrational energy is rapidly redistributed among low-frequency modes showing no Franck−Condon activity in the S_0-S_1 spectrum. $\Delta v = 0$ transitions from these dark states to the S_1 state and subsequent ionization can then take place in the vibrationally hot molecule. In contrast with ion-dip experiments, this technique is not isomer selective: the fact that only one ν(OH) vibration is observed in the non resonant spectrum confirms that there is only one isomer in our experimental conditions.

We can distinguish two regions in the spectrum recorded with the free electron laser: the region of the ν(CO) stretch vibration located at 1762 cm^{-1} and the fingerprint region where other vibrational frequencies located at 1297, 1125, 1001, and 735 cm^{-1} are associated with skeleton deformations.

2. Complexes between Methyl Mandelate and Methyl Lactate. By using pure enantiomers of each partner we are able to record separately the excitation spectra of each diastereoisomer. Figure 1b and 1c present the excitation spectra of the heterochiral (**RS**) and homochiral (**RR**) mixture of methyl mandelate and methyl lactate in the region of the methyl mandelate $S_0 \rightarrow S_1$ transition. The transition origin of methyl mandelate is strongly quenched by adding the methyl lactate. The spectra of the complexes show a blue shift of the origin transition relative to that of isolated methyl mandelate, which is usually assigned to a decrease of electrostatic forces upon electronic excitation.[35] The shift observed for the homochiral complex (+11 cm^{-1}) is larger than that of the heterochiral complex (+4 cm^{-1}). The **RS** and **RR** complexes probably have a similar structure since their excitation spectra are similar.

The IR/UV depletion spectra have been recorded in the range of the ν(OH) stretch mode with the probe set on the origin of the heterochiral and homochiral complex transition (Figure 3h and 3i, respectively). The vibrational spectrum of the **RS** complex displays two main bands at 3484 and 3528 cm^{-1} together with a smaller one at 3557 cm^{-1}. Two main bands at 3501 and 3535 cm^{-1} are also observed for the **RR** complex. They are accompanied by two weaker bands higher in energy by 11 and 24 cm^{-1} relative to the 3535 cm^{-1} transition. These bands as well as the small one in the spectrum of the **RS** complex are assigned to combination bands involving the methyl hindered rotation. The ν(OH) vibrational transitions of the **RR** complex are less shifted down in energy relative to the bare molecules than that of the **RS** complex; the hydrogen bonds at play in the latter complex should be slightly stronger. It is worth noticing that these values are lower than the frequency of the OH stretch mode in isolated methyl lactate (3565 cm^{-1}) and methyl mandelate (3565 cm^{-1}), which shows that the hydrogen bonds formed are stronger than the intramolecular hydrogen bonds existing in the isolated molecules.

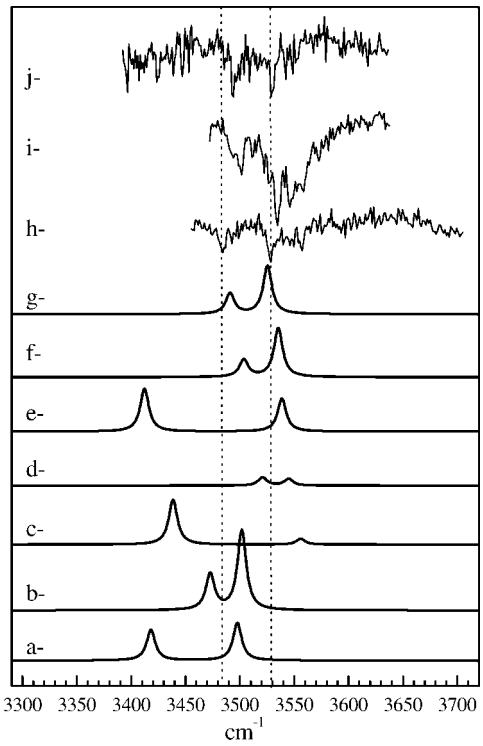

Figure 3. Experimental and theoretical IR spectra of complexes: (a−f) calculated IR spectra of **RS** methyl mandelate/methyl lactate diastereoisomer for (a) **RS**C5a$_{SsC}$folded, (b)**RS**C8a, (c) **RS**OH···OH$_{SsC}$, (d) **RS**-stacked, (e) **RS**C5a$_{GskC}$folded, (f) **RS**C5i$_{GskC}$, and (g) RSC5i$_{G'sk'C}$ and experimental spectra of (h) **RS** methyl mandelate/methyl lactate diastereoisomer, (i) **RR** methyl mandelate/methyl lactate diastereoisomer, and (j) methyl mandelate/methyl glycolate complex.

3. Complexes between Methyl Mandelate and Methyl Glycolate. The same experiment is done with methyl glycolate as a complexing agent for the sake of comparison with a nonchiral analogue. The excitation spectrum of the complex in the region of the S_0-S_1 origin transition of methyl mandelate is presented in Figure 1d. Besides the 0^0_0 transition of the isolated mandelate located at 37 503 cm^{-1}, an intense band appears at 37 515 cm^{-1} corresponding to the 0^0_0 transition of the methyl mandelate/methyl glycolate complex. Weaker lines appear at 37 533, 37 548, and 37 566 cm^{-1} and are the manifestation of low-frequency modes activity. We observe a blue shift (+12 cm^{-1}) of the origin band like in the previous case.

An IR/UV depletion spectrum is recorded in the range of the ν(OH) stretch mode. The probe is fixed at 37 515 cm^{-1} (Figure 3j). We observe two main bands at 3494 and 3528 cm^{-1}, which indicates that the geometry of this complex is similar to that of the methyl mandelate/methyl lactate complexes.

IV. Theoretical Results

1. Isolated Molecules. The methyl lactate molecule has already been studied[1,10,36−41] and is named after a three-letter nomenclature, which describes the conformation adopted by the H−O−C−C, O−C−C═O, and O═C−O−CH$_3$ dihedral angles. All previously conducted studies are in agreement and show that the main observed conformer is the same in a matrix,[36] in the gas phase[10,37] or in solution.[41] It is the so-called SsC species depicted in Figure 4a which shows an intramolecular OH···O═C hydrogen bond. S, s, and C stand for Syn, syn, and Cis and correspond to H−O−C−C, O−C−C═O, and O═C−O−CH$_3$ dihedral angles, respectively, which are all near 0°. Species in a much minor abundance, showing an OH···O$_{ester}$ hydrogen bond, have also been evidenced in matrix isolation IR spectroscopy experiments.[36] Following the previously described notation, they are named GskC and G′sk′C (Figure 4b and 4c, respectively). G and G′ stand for Gauche (H−O−C−C around 60° and −60°), while sk and sk′ stand for skew (O−C−C═O around 150° and −150°). Their population is less than 5% at room temperature. However, as complexation may favor conformers of minor abundance, they have been taken into account in the calculations which follow. The rotational barrier between these two conformers has been evaluated to be around 0.5 kcal/mol.[36] The population of all other conformers has been estimated to be zero, so they are not taken into account in this study. The energies of GskC and G′sk′C conformers relative to the most stable SsC conformer are 2.20 (1.74) and 2.39 (1.90) kcal/mol, respectively, at the B3LYP/6-31G(d,p) (MP2/6-31G(d,p)) level of theory.

The methyl glycolate molecule has also been studied by Fausto et al.[42] The conformers described in this paper are named following a two-letter nomenclature which describes the conformation adopted by the H−O−C−C and O−C−C═O dihedral angles. The most stable conformer is called Ss, where S and s stand for Syn and syn, respectively, which means that H−O−C−C and O−C−C═O dihedral angles are near 0°. The second conformer is degenerated by symmetry Gsk conformer (Gauche-skew, point group: C1) exhibiting H−O−C−C and O−C−C═O dihedral angles of 48.5° and 155.08°, respectively. The population of the Ss and Gsk conformers at room temperature represents 92% and 5%, respectively.

In this work, two isomers of the methyl mandelate molecule have been calculated at the MP2/6-31G(d,p) level of theory. The geometries are given in Figure 4d and 4e. They correspond to the SsC and G′sk′C configuration of methyl lactate with the methyl group replaced by a phenyl ring. They are separated by 1.6 kcal/mol, which means that the respective population of SsC and G′sk′C, at room temperature should be around 93% and 7% according to the Boltzmann distribution. It is to be noticed that no equivalent of the GskC conformer of methyl lactate is found in methyl mandelate due to the bulkiness of the benzene ring.

The harmonic vibrational frequencies are calculated at the B3LYP/6-31G(d,p) level. The frequencies are not scaled in the fingerprint and in the CO stretch regions of the spectra given in Figure 2, while a scaling factor of 0.96 is used in the OH/CH stretch region.[43,44] In the next paragraphs, frequencies will be given according to this scaling scheme. Frequencies of interest are given in Table 1.

Both conformers of methyl mandelate exhibit an intramolecular hydrogen bond directed from the hydroxyl to the carbonyl group in the SsC conformer and from the hydroxyl to the ester group in the G′sk′C conformer. The strength of the intramolecular hydrogen bond is larger in SsC than in G′sk′C, which manifests itself by a lower value (3551 cm^{-1}) of the calculated OH stretch frequency in SsC relative to 3644 cm^{-1} for the G′sk′C conformer. The CO stretch frequency is also slightly affected by the strength of the intramolecular hydrogen bond as its value is 1806 cm^{-1} for the SsC conformer and 1831 cm^{-1} for G′sk′C. The CH stretching mode localized on the asymmetric carbon is also conformation dependent. In the G′sk′C conformer its value (2956 cm^{-1}) is typical of an aliphatic CH stretch vibration, while in the SsC conformer it is shifted to the red by 55 cm^{-1} compared with the former one. The calculated frequencies of the OH and CH stretches located on the asymmetric carbon are therefore clearly different. Compari-

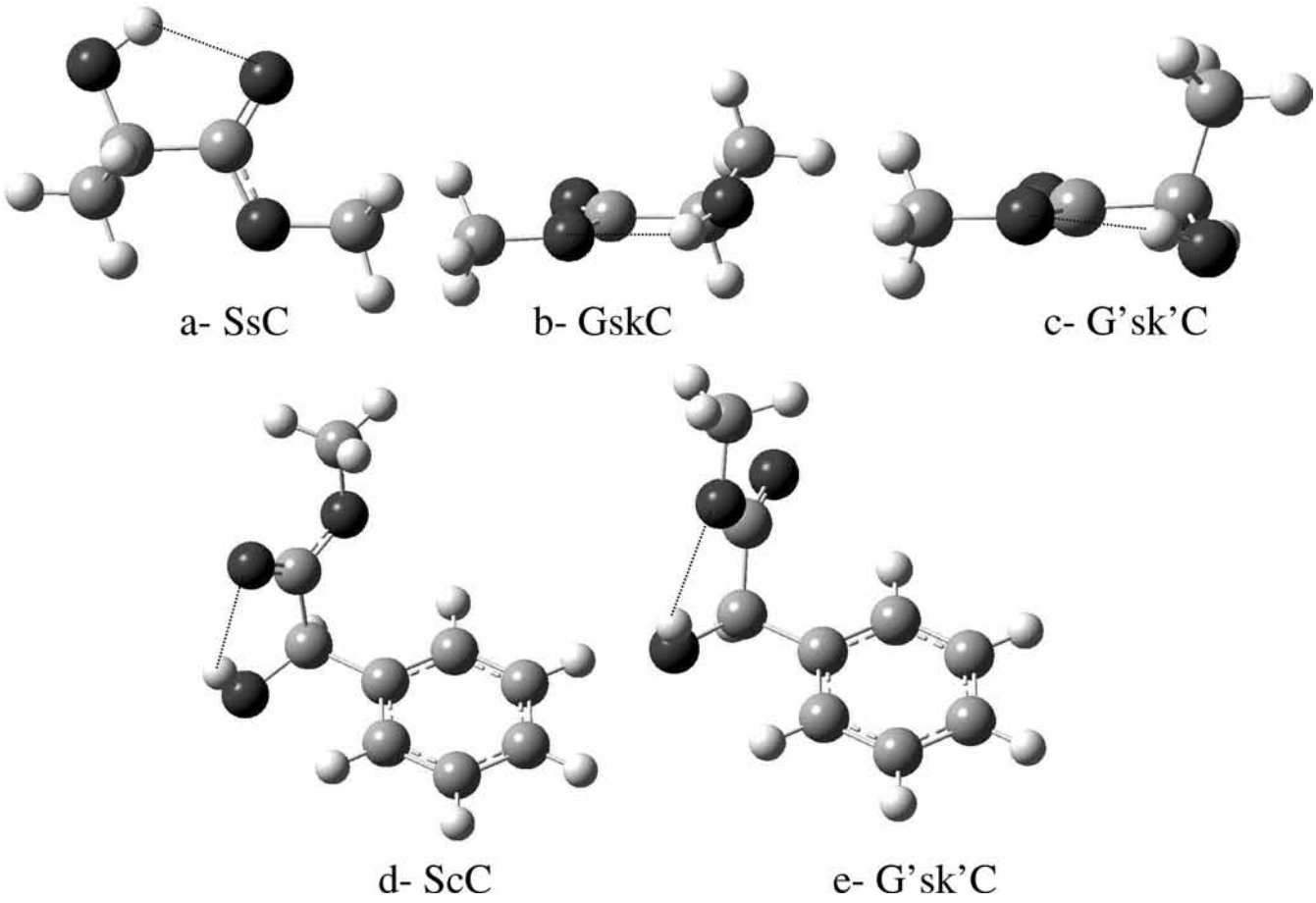

Figure 4. Geometries of bare molecules (a) SsC methyl lactate, (b) GskC methyl lactate, (c) G′sk′C methyl lactate, (d) SsC methyl mandelate, and (e) G′sk′C methyl mandelate.

TABLE 1: Vibrational Frequencies of the SsC and G′sk′C Conformers of Methyl Mandelate Calculated at B3LYP/6-31G(d,p) Level of Theory[a]

	SsC			G′sk′C			
	ν cm^{-1}			ν cm^{-1}			$\Delta\nu$ cm^{-1}
vibration localization	unscaled	scaled	*I*, km/mol	unscaled	scaled	*I*, km/mol	scaled
	1241		55	1291		155	
	1301		343	1263		151	
	1319		41	1292		94	
C═O	1806		204	1831		168	−25
CH asymmetric	3022	2901	22	3079	2956	9	−55
CH3s	3071	2948	27	3070	2948	29	1
CH3as	3153	3027	17	3152	3025	17	1
CHaromatic	3177	3050	1	3178	3051	0	−1
CH3as	3184	3057	11	3181	3054	13	3
CHaromatic	3185	3058	5	3188	3060	14	−2
CHaromatic	3194	3067	28	3199	3071	18	−5
CHaromatic	3205	3077	22	3207	3079	15	−2
CHaromatic	3220	3092	6	3218	3089	7	2
OH	3699	3551	98	3796	3644	42	−93

[a] The scaling factor used for the CH and OH stretch modes is 0.96; no scaling factor is applied to lower frequencies. The $\Delta\nu$ calculated corresponds to the shift of the vibration considered between the two conformers.

son with the experimental spectra allows us to assign the observed isomer to the most stable calculated SsC conformer.

Despite its similarity with methyl lactate, only one conformer of methyl mandelate is used as a starting point for the calculations. Indeed, only one conformer is observed in the experiment, whose origin transition is quenched by addition of methyl lactate. It is therefore likely that the experimentally observed complexes are built from this form. Thus, the calculations of the complexes are done starting from this most stable conformer.

2. Complexes. The methodology followed for the exploration of the whole potential-energy surface is described in detail in the Supporting Information. In what follows, we will describe the most stable calculated complexes following a structural organization nomenclature and give the energies DE as calculated at the B3LYP/6-31G(d,p) level of theory (Table 2). We

TABLE 2: Dissociation and Deformation Energies of the Complexes between *R*-Methyl Mandelate and *S*-Methyl Lactate[a]

	D_0	D_0 + 50% BSSE	E_{def} methyl mandelate	E_{def} methyl lactate	νOH, cm^{-1}	νOH, cm^{-1}
RSC8a*	8.13	**5.38**	3.87	2.88	3473	3502
RSC8b	7.10	**4.68**	3.08	2.94	3469	3524
RSC5a_{GskC}*	8.06	**5.77**	3.13	0.63	3419	3499
RSC5$i_{G'sk'C}$*	7.27	**5.28**	0.39	0.93	3491	3525
RSC5$i_{G'sk'C}$bis	7.04	**4.81**	0.45	0.69	3472	3550
RSC5i_{GskC}*	7.72	**5.15**	0.68	1.63	3504	3535
RSC5a_{GskC}folded*	7.65	**5.13**	2.22	0.48	3412	3539
RSC5i_{SsC}*	6.62	**4.30**	1.08	2.35	3468	3511
RSC5a_{SsC}	6.08	**3.90**	2.64	1.06	3404	3539
RSC5$_{SsC}$folded	5.74	**2.93**	2.34	1.05	3418	3498
RS-stacked*	6.23	**3.65**	0.27	0.23	3521	3545
RSOH···$_{SsC}$*	5.99	**3.70**	1.87	0.24	3439	3556
RSOH$_{GskC}$···OH	6.22	**4.40**	0.17	1.21	3483	3513
RSOH$_{G'sk'C}$···OH	5.86	**4.22**	0.17	0.52	3495	3520
RSOH···O=C$_{SsC}$	5.43	**3.19**	2.11	0.25	3487	3586
RSOH$_{G'sk'C}$···O=C	6.43	**4.14**	0.28	0.98	3543	3564
RS-bifurcated	6.56	**4.29**	0.23	0.34	3549	3590

[a] Dissociation energies as well as deformation energies are given in kcal/mol and calculated relative to the closest stable fragment. The energies of GskC and G′sk′C conformers relative to the most stable SsC conformer at this level of theory are 2.20 and 2.39 kcal/mol, respectively. All calculations were performed at the B3LYP/6-31G(d,p) level. Complexes marked with an asterisk are those which are discussed in Section IV.3.a. Details of nomenclature are given in the text Section IV.2.

will concentrate on the **RS** diastereoisomer because the results on **RR** diastereoisomers parallel those obtained for of the **RS**. Seventy two **RS** diastereoisomers have been calculated, which have been classified following their hydrogen-bond pattern.

a. C5 and C8 Structures. In our work, two stable C8 structures, **RS**C8a and **RS**C8b with dissociation energy of 5.38 and 4.68 kcal/mol, respectively, are identified for methyl mandelate/methyl lactate complexes. Both are based on the SsC conformers of both methyl lactate and methyl mandelate. The C8 structures based on GskC and G′sk′C conformers of methyl lactate are not calculated. They are expected to be much less stable than that with the SsC conformer of methyl lactate by analogy with the results obtained for the methyl lactate dimers.[28] The **RS**C8a structure is more stable than **RS**C8b by 0.7 kcal/mol. The main difference between both geometries is the way the intramolecular hydrogen bond opens up. In the **RS**C8b structure, the hydrogen of the methyl mandelate (methyl lactate) hydroxyl group is in a gauche (trans) position relative to the carbon of the phenyl ring (methyl group) attached to the asymmetric carbon, while it is in a trans (gauche) position in the **RS**C8a (Figure 5a) complex. As the steric hindrance is larger for phenyl than for methyl, we can explain the difference in dissociation energy by the fact that the phenyl group hinders formation of the C8 membered ring in the **RS**C8b complex more than the methyl does in **RS**C8a.

The most stable C5 structure corresponds to the **RS**C5a_{GskC} geometry (where a stands for the acceptor role of methyl mandelate), the dissociation energy of which is 5.77 kcal/mol. It is obtained by inserting the hydroxyl group of the methyl lactate GskC conformer into the SsC conformer of methyl mandelate. The intramolecular hydrogen bond of methyl mandelate is disrupted to allow insertion of the hydroxyl group of methyl lactate (see Figure 5b).

The **RS**C5$i_{G'sk'C}$ geometry (where i stands for insertion of methyl mandelate) corresponds to the opposite situation, where the hydroxyl group of methyl mandelate is inserted within the intramolecular hydrogen bond of methyl lactate in its G′sk′C conformer. Its dissociation energy is equal to 5.28 kcal/mol, and its geometry is depicted in Figure 5c. The **RS**C5$i_{G'sk'C}$ bis structure is very similar to the previous one; the difference in dissociation energies (4.81 kcal/mol compared with 5.28 kcal/mol) can be explained by formation of a less tightened ring. Actually, while the hydrogen bond between the OH group of methyl lactate and the OH group of methyl mandelate is similar in both complexes, the hydrogen bond between the OH and OCH_3 group of methyl lactate is looser in the second geometry (for **RS**C5$i_{G'sk'C}$ $d_{O\underline{H}\cdots\underline{O}H} = 1.90$Å, $\Theta_{OH\cdots O} = 166°$, $d_{O\underline{H}\cdots\underline{O}ester} = 2.11$Å, $\Theta_{OH\cdots Oester} = 135°$; for **RS**C5$i_{G'sk'C}$bis $d_{O\underline{H}\cdots\underline{O}H} = 1.87$Å, $\Theta_{OH\cdots O} = 158°$, $d_{O\underline{H}\cdots\underline{O}ester} = 2.46$Å, $\Theta_{OH\cdots Oester} = 119°$).

An equivalent structure is obtained with the GskC conformer of methyl lactate. It is denoted **RS**C5i_{GskC}, and its dissociation energy amounts to 5.15 kcal/mol. The main structural difference between **RS**C5i_{GskC} and **RS**C5$i_{G'sk'C}$ is related to the position of the methyl lactate molecule relative to the phenyl group of methyl mandelate. For **RS**C5i_{GskC} they are located on the same side of the lactate plane of methyl mandelate, while for the **RS**C5$i_{G'sk'C}$, they are on opposite sides of this plane.

The last C5a structure found with the GskC conformer of methyl lactate is **RS**C5a_{GskC}folded (DE = 5.13 kcal/mol). In contrast with the structures previously described, the lactate pattern of the methyl lactate arranges itself to lie above the phenyl ring of methyl mandelate, leading to the geometry depicted Figure 5d.

The **RS**C5i_{SsC} geometry (DE = 4.30 kcal/mol) corresponds to a C5 ring where the hydroxyl group of methyl mandelate inserts within the intramolecular hydrogen bond of the SsC conformer of methyl lactate. The opposite situation, where the hydroxyl group of methyl lactate inserts within the intramolecular hydrogen bond of the methyl mandelate, corresponds to the **RS**C5a_{SsC} complex, the dissociation energy of which is lower by 0.40 kcal/mol than that of the **RS**C5i_{SsC} complex. It is to be noticed that for the **RS**C5a_{SsC} complex the deformation energy of the methyl mandelate (2.64 kcal/mol) is higher than that of methyl lactate (2.35 kcal/mol) in the **RS**C5i_{SsC}, which seems to indicate that it is easier to open the methyl lactate than the methyl mandelate molecule in their ScC configurations. Finally, we also take into consideration the **RS**C5a_{SsC}folded complex, despite its small dissociation energy (DE = 2.93 kcal/mol). As the methyl lactate molecule is folded over the phenyl ring of methyl mandelate, its dissociation energy should gain a lot from MP2 calculations.

b. Stacked Geometry. The **RS-**stacked complex (Figure 5e) has been calculated starting from the SsC conformers of both methyl mandelate and methyl lactate. Its dissociation energy is 3.65 kcal/mol. The two lactate molecular planes lie parallel to each other, the methyl group of methyl lactate being as far as possible from the phenyl ring of methyl mandelate. For this geometry, none of the intramolecular hydrogen bonds is disrupted, which explains the low deformation energy calculated for each of the subunits.

c. OH···OH Geometries. This kind of structure involves the opening of the intramolecular bond of one of the subunits to allow formation of an intermolecular hydrogen bond from the hydroxyl group of the "opened" molecule to the hydroxyl group of the "closed" molecule. They have been found with the three conformers of methyl lactate and will be denoted hereafter **RS**OH···OH$_{conformer_name}$ when the methyl lactate

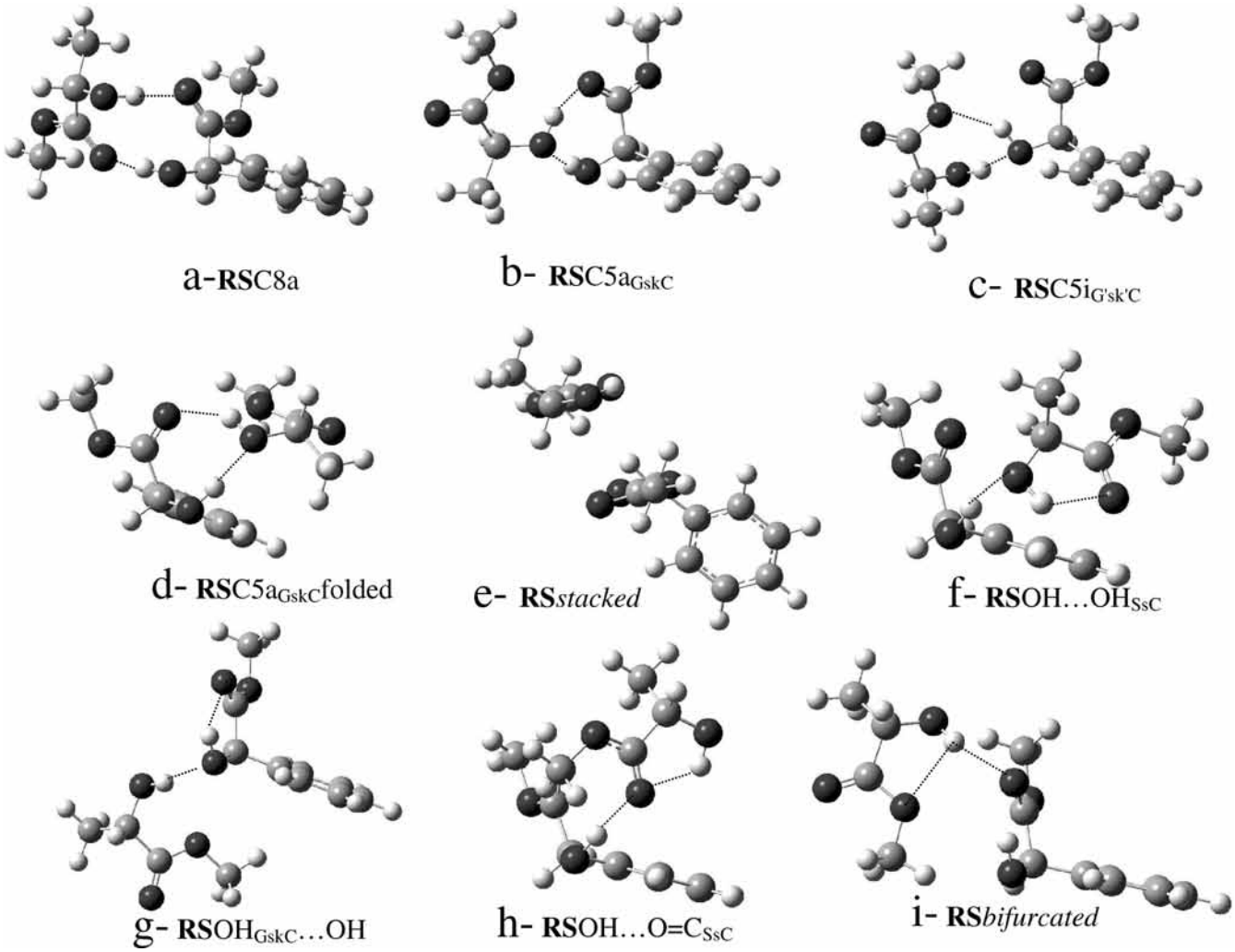

Figure 5. Geometries of **RS** methyl mandelate/methyl lactate diastereoisomers: (a) **RS**C8a, (b) **RS**C5a$_{GskC}$, (c) **RS**C5i$_{G'sk'C}$, (d) **RS**C5a$_{GskC}$ folded, (e) **RS**-stacked, (f) **RS**OH···OH$_{SsC}$, (g) **R**OH$_{GskC}$···OH, (h) **RS**OH···O=C$_{SsC}$, and (i) **RS**-bifurcated. See text for notations.

is the acceptor of the intermolecular hydrogen bond and **RS**OH$_{conformer_name}$···OH when it is the donor.

The **RS**OH···OH$_{SsC}$ complex corresponds to the opening of the intramolecular hydrogen bond of methyl mandelate and formation of an intermolecular hydrogen bond between the two hydroxyl groups of the system. Its dissociation energy is 3.70 kcal /mol. In this case, methyl lactate is in its SsC conformation (Figure 5f) and the methyl lactate molecule lies very close to the aromatic ring of methyl mandelate. Conversely, the complexes formed with both GskC and G′sk′C conformers of methyl lactate involve opening of the intramolecular hydrogen bond of methyl lactate to allow formation of the intermolecular hydrogen bond between the two hydroxyl groups of the system. They are referred to as **RS**OH$_{GskC}$···OH and **RS**OH$_{G'sk'C}$···OH in Table 2; their dissociation energies amount to 4.40 and 4.22 kcal/mol, respectively. The **RS**OH$_{GskC}$···OH geometry is given in Figure 5g.

d. OH···O=C and Bifurcated Geometries. Another family of complexes found in this study is that involving formation of an intermolecular hydrogen OH···O=C bond and concomitant opening of the intramolecular hydrogen bond of one of the two partners. Such conformers have been found for the complexes between methyl mandelate and the SsC and the G′sk′C conformers of methyl lactate. In the first case, the geometry is named **RS**OH···O=C$_{SsC}$, which means that the intramolecular hydrogen bond of methyl mandelate is disrupted to bind via an intermolecular hydrogen bond toward the carbonyl group of methyl lactate (Figure 5h). Its dissociation energy is equal to 3.19 kcal/mol. In the second case, **RS**OH$_{G'sk'C}$···O=C, the intramolecular hydrogen bond of the G′sk′C conformer of methyl lactate is opened to allow formation of the intermolecular hydrogen bond with the C=O group of methyl mandelate. Its dissociation energy amounts to 4.14 kcal/mol.

Finally, formation of the **RS**-bifurcated (Figure 5i) complex, obtained with the G′sk′C conformer of methyl lactate, involves no real opening of the intramolecular hydrogen bond. However, it is to be noticed that the hydroxyl group, even if already involved in an intramolecular hydrogen bond, is still able to make a second intermolecular hydrogen bond with the carbonyl group of methyl mandelate. It leads to a bifurcated hydrogen bond.[45,46] Its dissociation energy is 4.29 kcal/mol.

e. MP2 Optimizations. We will now concentrate on the most stable complexes in each structural family, i.e., **RS**C8a, **RS**C5a$_{GskC}$, **RS**C5i$_{G'sk'C}$, **RS**C5i$_{GskC}$, **RS**C5a$_{GskC}$folded, **RS**C5i$_{SsC}$, **RS**-stacked, **RS**OH···OH$_{SsC}$, and **RS**C5a$_{SsC}$folded. The **RS**C8b is not taken into account in what follows because steric hindrance makes it less stable than **RS**C8a. The structural similarity of **RS**C5i$_{G'sk'C}$bis and **RS**C5i$_{G'sk'C}$ makes us consider that only one them may be observed experimentally. The **RS**-bifurcated complex is also discarded because it is less stable than other **RS** complexes with the G′sk′C conformer of methyl lactate.

TABLE 3: Binding and Deformation Energies of Complexes between Methyl Mandelate and Methyl Lactate[a]

	ΔE_{mp2}	$\Delta E_{mp2} + \Delta ZPE_{mp2}$				
RMetlac$_{SsC}$	0.00	0.00				
RMetlac$_{GskC}$	1.72	1.74				
RMetlac$_{G'sk'C}$	1.90	1.90				
	De_{mp2}	**De_{mp2} + 50% BSSE**	E_{def} 1a	E_{def} Methlac	ν_{OH} cm^{-1}	ν_{OH} cm^{-1}
RSC5a$_{SsC}$folded	13.53	**9.09**	2.16	0.86	3418	3498
RSC8a	13.03	**9.01**	3.51	3.03	3473	3502
RSOH$\cdots$OH$_{SsC}$	12.58	**8.73**	1.83	0.21	3439	3556
RSC5i$_{SsC}$	10.98	**7.86**	0.86	2.01	3468	3511
RS-stacked	11.35	**7.72**	0.35	0.23	3521	3545
RSC5a$_{GskC}$folded	14.96	**10.63**	1.98	0.35	3412	3539
RSC5i$_{GskC}$	12.78	**9.11**	0.69	1.89	3504	3535
RSC5a$_{GskC}$	11.76	**8.50**	2.30	0.54	3419	3499
RSC5i$_{G'sk'C}$	11.02	**8.29**	0.30	1.05	3491	3525
experimental (**RS**)					3484	3528
RRC5a$_{SsC}$folded	14.26	**9.80**	1.94	0.41	3399	3501
RRC8a	13.72	**9.12**	4.01	3.48	3475	3507
RROH$\cdots$OH$_{SsC}$	12.23	**8.73**	1.98	0.42	3422	3532
RRC5i$_{SsC}$	11.63	**7.83**	0.50	3.64	3438	3512
RRstacked	11.40	**7.80**	0.32	0.23	3523	3560
RRC5a$_{G'sk'C}$folded	14.96	**10.66**	2.02	0.34	3411	3532
RRCi5$_{G'sk'C}$	13.28	**9.52**	0.75	1.33	3502	3537
RRC5i$_{GskC}$	10.84	**7.76**	0.34	0.85	3489	3530
RRC5a$_{GskC}$	10.53	**7.34**	2.37	0.55	3407	3545
experimental (**RR**)					3501	3535

[a] Energies are given in kcal/mol and calculated relative to the closest stable fragment. All calculations were performed at the MP2/6-31G(d,p). Details of nomenclature are given in Section IV.2.

These structures have been reoptimized at the MP2 level of theory. The main result (Table 3) of these calculations is that three structures (**RS**C5a$_{GskC}$folded, **RS**C5a$_{SsC}$folded, and **RS**OH$\cdots$OH$_{SsC}$) are highly stabilized compared to the others because they involve important dispersion interactions between the aromatic ring of methyl mandelate and the lactate plane of methyl lactate. Moreover, the **RS**C5i$_{G'sk'C}$ and **RS**C5i$_{GskC}$ structures differ much more in binding energy at the MP2 than at the DFT level because dispersion interactions are larger when the phenyl ring of methyl mandelate and the methyl lactate molecules are on the same side of the lactate plane of methyl mandelate than when they are opposite relative to this plane.

3. Assignment. ***a. Complexes between Methyl Mandelate and Methyl Lactate.*** We will now discuss the above-mentioned structures in terms of their suitability as candidates for the observed complex. We will consider first the complexes formed with the SsC conformer of methyl lactate and then those with the GskC and G′sk′C conformers. We will discuss them first in terms of binding energy and comparison between calculated and experimental frequencies.

The three most stable complexes obtained with the SsC conformers of methyl lactate and methyl mandelate are almost isoenergetic. **RS**C5a$_{SsC}$folded becomes the most stable one after MP2 reoptimization. Its binding energy amounts to 9.09 kcal/mol. Unfortunately, its infrared spectrum in the range of the OH stretches (Figure 3a) does not fit the experimental results at all, one of the two OH vibrations, located at 3418 cm^{-1}, being too red shifted. We can therefore safely exclude that this complex corresponds to the experimentally observed structure. The second most stable form is the **RS**C8a geometry. Its binding energy is equal to 9.01 kcal/mol, and its spectrum (Figure 3b) displays two vibrational frequencies located at 3473 and 3502 cm^{-1}, which makes it a possible candidate for the observed complex, whose experimental stretch frequencies are 3484 and 3528 cm^{-1}. The third complex involving the SsC conformer of methyl lactate is the **RS**OH$\cdots$OH$_{SsC}$ complex (BE = 8.73 kcal/mol). This latter complex is also largely stabilized during reoptimization at the MP2 level of theory because the methyl lactate molecule is lying above the phenyl ring of methyl mandelate, which implies high dispersion interactions. Its calculated vibrational frequencies are located at 3439 and 3556 cm^{-1}, and the 117 cm^{-1} gap between them appears to be too large compared to the 44 cm^{-1} experimental value (Figure 3c). We therefore rule out the hypothesis that this complex could be the experimentally observed form.

The **RS**C5i$_{SsC}$ and the **RS**-stacked complexes have lower binding energies (7.86 and 7.72 kcal/mol, respectively) than those described above, which allows us to discard them. Owing to these results on binding energies as well as calculated vibrational frequencies it seems that **RS**C8a has the highest chance to be observed among those built from the SsC conformer of methyl lactate.

The most stable calculated complex between methyl mandelate and one of the GskC and G′sk′C conformers of methyl lactate is **RS**C5$_{GskC}$folded. Its binding energy amounts to 10.63 kcal/mol. Its relative binding energy has increased a lot in MP2 calculations because, as in the case of the **RS**OH$\cdots$OH$_{SsC}$ or **RS**C5a$_{GskC}$folded complexes, the methyl lactate molecule lies above the phenyl ring of methyl mandelate. Its calculated spectrum (Figure 3e) displays frequencies located at 3412 and 3539 cm^{-1}; the 3412 cm^{-1} value appears to be too red shifted compared with the experimental one (3484 cm^{-1}), and the gap of 127 cm^{-1} between these frequencies is really too large relative to the experimental one (44 cm^{-1}). Thus, we think that this complex is not observed in our experimental conditions. The following complex, in terms of binding energy, corresponds to the **RS**C5i$_{GskC}$ structure. It also gains in stability from MP2 calculation because methyl lactate lies at the edge of the phenyl ring of methyl mandelate. Its binding energy equals 9.11 kcal/mol. The calculated vibrational frequencies are located at 3504 and 3535 cm^{-1}; they make this structure a possible complex to explain the experimental spectrum observed (Figure 3f). The two last structures have lower binding energies, 8.50 and 8.29 kcal/mol for **RS**C5a$_{GskC}$ and **RS**C5i$_{G'sk'C}$, respectively. The spectrum of the **RS**C5a$_{GskC}$ displays OH stretch frequencies located at 3419 and 3499 cm^{-1}. The gap between these frequencies is 80 cm^{-1} and does not correspond to the experimental one which is 44 cm^{-1}. The calculated spectrum of **RS**C5i$_{G'sk'C}$ (Figure 3g), with bands located at 3491 and 3525 cm^{-1}, seems to fit the best the experimental frequencies, which allows us to keep this structure for the final discussion.

Thus, at the end we are left with the **RS**C8a, **RS**C5i$_{GskC}$, and **RS**C5i$_{G'sk'C}$ structures for the **RS** diastereoisomer. By playing the same game with the 70 complexes calculated for the **RR** diastereoisomer we are also left with three structures: **RR**C8a, **RR**C5i$_{GskC}$, and **RR**C5i$_{G'sk'C}$.

Now we can go a little further by considering that the complexes observed in our experiment must involve relatively low deformation energy. That means that the cooling process is mainly kinetically controlled. Experimental studies[47] of the cooling process in a supersonic expansion seeded with inert gas indicate that under the conditions used here relaxation of conformers is complete if the barrier for isomerization is low enough (less than 400 cm^{-1} [1.2 kcal/mol]). The isomerization processes have also been taken into account by others, among which are Zwier et al.[48,49] and Godfrey et al.,[50,51] who determined lower limits of the isomerization barrier of the same order.

In what follows we do not want to apply a direct correspondence between deformation energy and isomerization barrier. Indeed, formation of complexes with huge deformation energies is possible when no energy barriers are involved.[52] However, we noticed from past experience that no complexes[11] or conformers[12] of molecules with an internal H bond are seen in our experimental conditions when the deformation energy is higher than 2 kcal/mol. In these cases the deformation (opening of an intramolecular hydrogen bond) has to occur somehow prior to complete complex formation, even if both processes are concerted under thermodynamically controlled conditions. Despite the relation between deformation energy and isomerization barrier being not direct, it should be the same for formation of similar complexes. Our study of the complexation of α-methyl-2-naphthalenemethanol by methyl lactate has unambiguously evidenced that the insertion complex displaying a deformation energy of 2.35 kcal/mol was not observed experimentally.[10] We want to point out that also for the molecular system described here we deduced from the comparison between calculated and experimental frequencies that we do not observe the stable calculated complexes **RS**C5a$_{GskC}$folded or **RS**OH···OH$_{SsC}$, whose deformation energy of methyl mandelate amounts to 1.98 and 1.83 kcal/mol, respectively. Keeping these data in mind, we propose a value of 1.8−2 kcal/mol as the deformation energy higher limit for a complex to be observed in our experimental conditions. Therefore, we can safely assume that the **RS**C8a structures which involves huge deformation energies (3.51 and 3.03 kcal/mol for methyl mandelate and methyl lactate, respectively) are not formed in our experimental setup. We propose that one of the **RS**C5i$_{G'sk'C}$ or **RS**C5i$_{GskC}$ structures is the complex responsible for the observed spectrum of the **RS** diastereoisomer. Moreover, the **RS**C5i$_{GskC}$ displays a deformation energy of 1.89 kcal/mol for the methyl lactate, which at the precision of the calculations is not so far from the 1.98 kcal/mol of **RS**C5a$_{GskC}$folded. Thus, we are inclined to attribute the observed infrared spectrum to the **RS**C5i$_{G'sk'C}$ geometry.

For the **RR** diastereoisomer, the attribution is somewhat easier. The **RR**C8a structure is excluded for the same reason as **RS**C8a; it involves huge deformation energies (4.01 and 3.48 kcal/mol for methyl mandelate and methyl lactate, respectively). Concerning the C5 structures, both **RR**C5i$_{G'sk'C}$ and **RR**C5i$_{GskC}$ have low deformation energies (below 1.33 kcal/mol) and the binding energy of **RR**C5i$_{G'sk'C}$ is clearly higher than that of **RR**C5i$_{GskC}$. Thus, we assign the **RR**C5i$_{G'sk'C}$ geometry to the complex responsible for the observed spectrum.

This attribution is also coherent with the fact that the vibrational frequencies of the **RS** diastereoisomer are more shifted down in energy relative to the bare molecules than those of the **RR** one. Actually, if we look at Figure 6 presenting the vibrational spectra of **RS**i$_{GskC}$ (Figure 6a), **RS**i$_{G'sk'C}$ (Figure 6b), **RR**i$_{GskC}$ (Figure 6d), and **RR**i$_{G'sk'C}$ (Figure 6e) we can notice that when both methyl lactate and phenyl groups are on opposite sides relative to the lactate plane of methyl mandelate (Figure 6b and 6d) the calculated frequencies are more red shifted than when the methyl lactate and phenyl group are the same side (Figure 6a and 6e). This can be explained through a subtle balance between dispersion and electrostatic forces. When methyl lactate is near the phenyl (**RS**i$_{GskC}$ or **RR**i$_{G'sk'C}$), dispersion between these two parts tends to be optimized to the prejudice of electrostatic interaction. As a result, the C5 ring is somewhat distorted. This contrasts with the reverse case (**RS**i$_{G'sk'C}$ or **RR**i$_{GskC}$) where the binding energy is optimized mainly upon C5 ring formation. This may explain why the associated frequencies are more red shifted in the latter case.

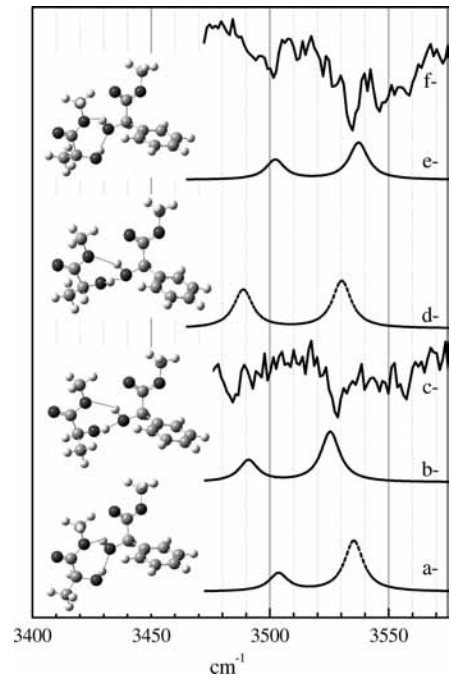

Figure 6. Experimental spectra for (c) **RS** methyl mandelate/methyl lactate diastereoisomer and (f) **RR** methyl mandelate/methyl lactate diastereoisomer associated the geometries and calculated spectra of complexes (a) **RS** C5i$_{GskC}$, (b) **RS** C5i$_{G'sk'C}$, (d) **RR** C5i$_{GskC}$, and (e) **RR** C5i$_{G'sk'C}$.

TABLE 4: Binding and Deformation Energies of Complexes between Methyl Mandelate and Methyl Glycolate Together with Calculated Frequencies Obtained at the B3LYP/6-31G(d,p) Level[a]

	ΔE_{mp2}	$\Delta E_{mp2} + \Delta ZPE_{mp2}$
Gly$_{Ss}$	0.00	0.00
Gky$_{Gsk}$	1.83	2.04

	De_{mp2}	**De_{mp2} + 50% BSSE**	E_{def} 1a	E_{def} Methlac	ν_{OH} cm^{-1}	ν_{OH} cm^{-1}
C5$_{Ss}$folded	14.03	**9.59**	1.97	0.42	3403	3498
C8	13.62	**9.17**	4.02	3.22	3465	3517
C5$_{Gsk}$folded	14.63	**10.40**	1.98	0.34	3421	3515
C5front	13.01	**9.46**	0.71	1.38	3501	3532
C5back	11.16	**8.01**	0.58	0.79	3481	3526
experimental					3494	3528

[a] Energies are given in kcal/mol and calculated relative to the closest stable fragment. All calculations were performed at the MP2/6-31G(d,p).

b. Complexes between Methyl Mandelate and Methyl Glycolate. The calculations for methyl mandelate/methyl glycolate complexes were performed starting from the previously calculated stable complexes of the **RS** diastereoisomer by replacing CH3 by H (Table 4). In what follows, C8 is related to **RS**C8a, C5a$_{Ss}$folded to **RS**C5a$_{SsC}$folded, C5a$_{Gsk}$folded to **RS**C5a$_{GskC}$folded, C5i$_{back}$ to **RS**i$_{G'sk'C}$, where glycolate and the phenyl ring are opposite each other relative to the lactate plane of methyl mandelate, and C5i$_{front}$ to **RS**i$_{GskC}$, where glycolate and the phenyl ring are on the same side of the lactate pattern of methyl mandelate. The most stable complex obtained by complexation of the Ss conformer of methyl glycolate with the SsC conformer of methyl mandelate is C5a$_{Ss}$folded (DE = 9.59 kcal/mol). Its calculated vibrational frequencies (3403 and 3498 cm^{-1}) do not fit the experimental values (3494 and 3528 cm^{-1}), and the deformation energy amounts to 1.97 for the methyl mandelate. All these results make this complex unlikely to be

formed. The C8 complex formed between methyl mandelate and the Ss conformer of methyl glycolate appears to be less stable than C5a_{Ss}folded. Its binding energy is lower by 0.42 kcal/mol. The calculated vibrational frequencies could be suitable even if the value of 3465 cm^{-1} is a little too red shifted compared to the experimental value (3494 cm^{-1}). However, its deformation energies are huge for both subunits (4.02 and 3.22 kcal/mol for methyl mandelate and methyl glycolate, respectively), which precludes formation of this complex in our experiment setup.

Now regarding complexes between methyl mandelate and the Gsk conformer of methyl glycolate, the most stable structure is the C5a_{Gsk}folded complex, with a binding energy amounting to 10.40 kcal/mol. The deformation energy of methyl mandelate is 1.98 kcal/mol, and the vibrational frequencies calculated for this structure are not suitable; they appear to be too red shifted compared with experimental values, and the gap between the OH frequencies is 94 cm^{-1}, which does not correspond to the experimental value (34 cm^{-1}). The following complex in terms of binding energy is the C5i_{front} complex. Its binding energy is 9.46 kcal/mol, and the deformation energies on methyl mandelate and methyl lactate are 0.71 and 1.38 kcal/mol, respectively. Moreover, the calculated vibrational frequencies are in good agreement with the experimental values by both their position and the gap between them. Thus, we assign this complex to the experimentally observed one. As was the case for the methyl mandelate/methyl lactate complexes, the C5i_{back} structure appears to be less stable (8.01 kcal/mol) than the C5i_{front} one because the methyl glycolate is far from the phenyl ring, which results in less dispersion interaction than in the latter complex. The choice between C5i_{back} and C5i_{front} is only made in terms of dissociation energies, as was the case for the **RR** methyl mandelate/methyl lactate complexes.

We even notice that the attributed complexes for the **RR** methyl mandelate/methyl lactate and methyl mandelate/methyl glycolate complexes are the same (**RR**C5$i_{G'sk'C}$ related C5i_{front}) and differ from that attributed to the **RS** methyl mandelate/methyl lactate complex (**RS**C5$i_{G'sk'C}$ related C5i_{back}). This may explain the fact that the shift of the electronic transition is similar for the **RR** methyl mandelate/methyl lactate and methyl mandelate/methyl glycolate complexes.

V. Comparison with Similar Systems: The Case of Methyl Lactate

The main characteristics of the methyl lactate and methyl glycolate dimers infrared spectrum can be summarized as follows.[1,13,53] The main observed feature is a very intense band, which appears slightly above 3500 cm^{-1}. This feature survives addition of argon in the expansion, which can be taken as an indication for a large stability of the corresponding adduct. Moreover, increasing the proportion of argon in the admixture results in the appearance of a new band slightly shifted to the red relative to the above-mentioned one, which has been assigned to an argon-coated dimer. On the basis of these experimental findings, this absorption band has been assigned to the most stable dimer, namely, the C8 form. An additional argument in favor of this assignment is the pseudo-centrosymmetric character of the complex, which justifies that all the oscillator strength is borne by one OH stretch mode. Comparison with the calculated frequencies of C8 supports this assignment. Bands of weaker intensity appear near the main band and could correspond to combination bands or C5 structures.

The methyl mandelate/methyl lactate or methyl mandelate/methyl glycolate complexes studied by laser-induced fluorescence and fluorescence dip IR spectroscopy clearly exhibit different behaviors. They only show one absorption band in the S_0-S_1 spectrum, which rules out the presence of more than one isomer in our experimental conditions. This complex has been assigned to a C5 structure, in contrast with the methyl lactate or methyl glycolate dimers, where the C8 form is dominant. The differences between the two sets of data can arise either from the nature of the molecules at play or from the cooling conditions.

In view of our results, we think that the nature of the molecules is not responsible for the differences shown previously. First, the intramolecular hydrogen bonds for the most stable form SsC of methyl lactate, methyl glycolate, and methyl mandelate are equivalent, which is evidenced by the OH stretch frequencies observed (3565, 3571, and 3565 cm^{-1}, respectively). Furthermore, in view of the calculations on the C8 conformers, it appears that the deformation energy needed to open the SsC conformer of methyl lactate and insert an hydroxyl group (about 2.9 kcal/mol) is almost as high as that needed for the SsC conformer of methyl mandelate (3−4 kcal/mol). This means that in similar experimental conditions, i.e., with the same processes governing formation of the complexes, the same type of structures should be formed for methyl lactate and methyl mandelate.

This leads us to consider that different cooling conditions are responsible for the different behaviors observed in both systems. The LIF experiments rest on the use of a pulsed axisymmetric nozzle with an opening time of about 200−400 μs. The FTIR experiments use a slit nozzle with an opening time on the order of 100−200 ms. Moreover, the pressure conditions are different in both experimental setups. In our experiments, the pressure in the expansion chamber is below 0.1 mbar for a backing pressure of 1 bar, while in the slit jet experiment with the same backing pressure the residual pressure is 4 mbar. This difference is linked to the relative size of the hole in our experiment and the size of the slit of the experiment of Borho et al. Actually, the equivalent diameter of the slit used in the filet-jet experiment is 40 times larger than that of the hole in our experiment. Another difference is the species concentration; in a slit jet the species density is proportional to $1/R$ (where R is the distance relative to the orifice of the expansion), while it is proportional to $1/R^2$ in a pinhole jet. Finally, the cooling process has been demonstrated to be slower for slit jet than for pinhole jet.[54] Thus, it appears that the cooling operates with a lower species density and a faster cooling for the pinhole jet experiments than in filet-jet experiments. All those differences are probably at the origin of different cooling processes.

Formation of a C5 complex requires less molecular reorganization than that of C8, which is quantified by the smaller deformation energy in C5, while the C5 total binding energy is lower than that of the C8 structure. As already described, only C5 structures are observed in our experiments; this indicates that the cooling process in our experiment is preferentially kinetically controlled. This contrasts with the results of Borho et al., who observed mainly C8 structures. This tends to indicate that the cooling conditions specific to the filet jet allows formation of complexes involving high deformation energy in contrast with our experiment. To reinforce the idea, we notice that these authors also evidenced easy formation of multimers up to the quadrimer. Indeed, the quadrimer has been shown to have a very high dissociation energy[14] due to a high cooperative hydrogen-bond network involving opening of all the intramolecular hydrogen bonds.

VI. Conclusions

We were able to observe chiral discrimination when complexing the R enantiomer of methyl mandelate with both R and S enantiomers of methyl lactate. Owing to the similarity of the hydrogen-bonded networks at play, the **RS** and **RR** complexes show similar 0^0_0 transition energies separated by only 7 cm^{-1}. These complexes are based on a C5 structure. However, more subtle effects result in different IR spectra. The infrared spectra show significantly different shifts of the OH vibration which are due to small geometry differences between the **RS** and **RR** diastereoisomers. The relative position of the methyl lactate molecule and the phenyl ring of methyl mandelate have been crucial to explain this difference in the IR spectra. When both methyl lactate (or methyl glycolate) and the phenyl ring are on the same side of the lactate molecular plane of methyl mandelate, the red shift of the OH stretch frequencies has been calculated to be smaller than when they are opposite relative to this plane. This result allows us to assign the **RR** complex to a structure in which the phenyl ring and methyl lactate molecule are on the same side of the plane defined by the intramolecular H bond of mandelate, while they are lying on opposite sides in the **RS** complex. The difference between the present results and those previously reported on methyl lactate dimers[1] is supposed to be due to the cooling process, which is preferentially kinetically controlled in our experiment, while the experiment of Borho et al. allows for formation of complexes with a larger deformation energy.

Acknowledgment. The authors would like to acknowledge support from the DI (Orsay University) for allotment of computer resources. Thanks are due to Dr. Corey RICE for his help during part of the experiments described here.

Supporting Information Available: Description of the exploration of the whole potential-energy surface together with all calculated complexes for both RR and RS diastereoisomers at the B3LYP/6-31G(d,p) level of theory. The complexes indicated in gray are those discussed in the text. This material is available free of charge via the Internet at http://pubs.acs.org.

References and Notes

(1) Borho, N.; Suhm, M. A. *Org. Biomol. Chem.* **2003**, *1*, 4351.
(2) Al Rabaa, A. R.; Breheret, E.; Lahmani, F.; Zehnacker, A. *Chem. Phys. Lett.* **1995**, *237*, 480.
(3) Al Rabaa, A.; Le Barbu, K.; Lahmani, F.; Zehnacker-Rentien, A. *J. Phys. Chem. A* **1997**, *101*, 3273.
(4) Le Barbu, K.; Brenner, V.; Millié, P.; Lahmani, F.; Zehnacker-Rentien, A. *J. Phys. Chem. A* **1998**, *102*, 128.
(5) Lahmani, F.; Le Barbu, K.; Zehnacker-Rentien, A. *J. Phys. Chem. A* **1999**, *103*, 1991.
(6) Mons, M.; Piuzzi, F.; Dimicoli, I.; Zehnacker, A.; Lahmani, F. *Phys. Chem. Chem. Phys.* **2000**, *2*, 5065.
(7) Le Barbu, K.; Lahmani, F.; Zehnacker-Rentien, A. *J. Phys. Chem. A* **2002**, *106*, 6271.
(8) Lahmani, F.; Le Barbu-Debus, K.; Seurre, N.; Zehnacker-Rentien, A. *Chem. Phys. Lett.* **2003**, *375*, 636.
(9) Seurre, N.; Le Barbu-Debus, K.; Lahmani, F.; Zehnacker-Rentien, A.; Sepiol, J. *J. Mol. Struct.* **2004**, *692*, 127.
(10) Seurre, N.; Le Barbu-Debus, K.; Lahmani, F.; Zehnacker, A.; Borho, N.; Suhm, M. A. *Phys. Chem. Chem. Phys.* **2006**, *8*, 1007.
(11) Seurre, N.; Sepiol, J.; Le Barbu-Debus, K.; Lahmani, F.; Zehnacker-Rentien, A. *Phys. Chem. Chem. Phys.* **2004**, *6*, 2867.
(12) Le Barbu-Debus, K.; Lahmani, F.; Zehnacker-Rentien, A.; Panja, S. S.; Chakraborty, T.; Guchhait, N. *J. Chem. Phys.* **2006**, *125*, 174305.
(13) Borho, N.; Suhm, M. A. *Phys. Chem. Chem. Phys.* **2004**, *6*, 2885.
(14) Adler, T. B.; Borho, N.; Reiher, M.; Suhm, M. A. *Angew. Chem., Int. Ed.* **2006**, *45*, 3440.
(15) Giuliano, B. M.; Ottaviani, P.; Favero, L. B.; Caminati, W.; Grabow, J. U.; Giardini, A.; Satta, M. *Phys. Chem. Chem. Phys.* **2007**, *9*, 4460.
(16) Page, R. H.; Shen, Y. R.; Lee, Y. T. *J. Chem. Phys.* **1988**, *88*, 4621.
(17) Riehn, C.; Lahmann, C.; Wassermann, B.; Brutschy, B. *Chem. Phys. Lett.* **1992**, *197*, 443.
(18) Tanabe, S.; Ebata, T.; Fujii, M.; Mikami, N. *Chem. Phys. Lett.* **1993**, *215*, 347.
(19) Pribble, R. N.; Zwier, T. S. *Science* **1994**, *265*, 75.
(20) Broquier, M.; Lahmani, F.; Zehnacker-Rentien, A.; Brenner, V.; Millie, P.; Peremans, A. *J. Phys. Chem. A* **2001**, *105*, 6841.
(21) Prazeres, R.; Berset, J. M.; Glotin, F.; Jaroszynski, D.; Ortega, J. M. *Nuclear Instrum. Methods Phys. Res., Sect. A* **1993**, *331*, 15.
(22) Le Barbu, K.; Lahmani, F.; Mons, M.; Broquier, M.; Zehnacker, A. *Phys. Chem. Chem. Phys.* **2001**, *3*, 4684.
(23) Claverie, P. *Intermolecular Interactions from diatomics to biopolymers*; Pullman, B., Ed.; Wiley: New York, 1978.
(24) Brenner, V.; Millié, P. *Z. Phys. D* **1994**, *30*, 327.
(25) Vigne-Mader, F.; Claverie, P. *J. Phys. Chem.* **1988**, *88*, 4934.
(26) Bockish, F.; Liotard, D.; Rayez, J. C. *Int. J. Quantum Chem.* **1992**, *44*, 619.
(27) Metropolis, N.; Rosenbluth, A.; Teller, A.; Teller, E. *J. Chem. Phys.* **1953**, *21*, 1087.
(28) Borho, N. Chirale Erkennung in Molekülclustern: Massgeschneiderte Aggregation von α-Hydroxyestern; Goettingen Universty: Goettingen, Germany, 2004.
(29) Frisch, M. J.; Trucks, G. W.; Schlegel, H. B.; Scuseria, G. E.; Robb, M. A.; Cheeseman, J. R.; Montgomery, J. A., Jr.; Kudin, T. V. K. N.; Burant, J. C.; Millam, J. M.; Iyengar, S. S.; Tomasi, J.; Barone, V.; Mennucci, B.; Cossi, M.; Scalmani, G.; Rega, N.; Petersson, G. A.; Nakatsuji, H.; Hada, M.; Ehara, M.; Toyota, K.; Fukuda, R.; Hasegawa, J.; Ishida, M.; Nakajima, T.; Honda, Y.; Kitao, O.; Nakai, H.; Klene, M.; Li, X.; Knox, J. E.; Hratchian, H. P.; Cross, J. B.; Adamo, C.; Jaramillo, J.; Gomperts, R.; Stratmann, R. E.; Yazyev, O.; Austin, A. J.; Cammi, R.; Pomelli, C.; Ochterski, J. W.; Ayala, P. Y.; Morokuma, K.; Voth, G. A.; Salvador, P.; Dannenberg, J. J.; Zakrzewski, V. G.; Dapprich, S.; Daniels, A. D.; Strain, M. C.; Farkas, O.; Malick, D. K.; Rabuck, A. D.; Raghavachari, K.; Foresman, J. B.; Ortiz, J. V.; Cui, Q.; Baboul, A. G.; Clifford, S.; Cioslowski, J.; Stefanov, B. B.; Liu, G.; Piskorz, A. L.; P.; Komaromi, I.; Martin, R. L.; Fox, D. J.; Keith, T.; Al-Laham, M. A.; Peng, C. Y.; Nanayakkara, A.; Challacombe, M.; Gill, P. M. W.; Johnson, B.; Chen, W.; Wong, M. W.; Gonzalez, C.; Pople, J. A. *Gaussian 03*, Revision C.02; Gaussian, Inc.: Wallingford, CT, 2004.
(30) Boys, S.; Bernardi, F. *Mol. Phys.* **1970**, *19*, 553.
(31) Kim, K. S.; Tarakeshwar, P.; Lee, J. Y. *Chem. Rev.* **2000**, *100*, 4145.
(32) Zielke, P.; Suhm, M. A. *Phys. Chem. Chem. Phys.* **2006**, *8*, 2826.
(33) Liu, Y. Q.; Rice, C. A.; Suhm, M. A. *Can. J. Chem., Rev. Can. Chem.* **2004**, *82*, 1006.
(34) Fujii, A.; Okuyama, S.; Iwasaki, A.; Maeyama, T.; Ebata, T.; Mikami, N. *Chem. Phys. Lett.* **1996**, *256*, 1.
(35) Seurre, N.; Sepiol, J.; Lahmani, F.; Zehnacker-Rentien, A.; Le Barbu-Debus, K. *Phys. Chem. Chem. Phys.* **2004**, *6*, 4658.
(36) Borba, A.; Gomez-Zavaglia, A.; Lapinski, L.; Fausto, R. *Vibr. Spectrosc.* **2004**, *36*, 79.
(37) Borho, N.; Suhm, M. A.; Le Barbu-Debus, K.; Zehnacker, A. *Phys. Chem. Chem. Phys.* **2006**, *8*, 4449.
(38) Ottaviani, P.; Velino, B.; Caminati, W. *Chem. Phys. Lett.* **2006**, *428*, 236.
(39) Aparicio, S. *J. Phys. Chem. A* **2007**, *111*, 4671.
(40) Borho, N.; Xu, Y. J. *Phys. Chem. Chem. Phys.* **2007**, *9*, 1324.
(41) Gigante, D. M. P.; Long, F. J.; Bodack, L. A.; Evans, J. M.; Kallmerten, J.; Nafie, L. A.; Freedman, T. B. *J. Phys. Chem. A* **1999**, *103*, 1523.
(42) Jarmelo, S.; Fausto, R. *J. Mol. Struct.* **1999**, *509*, 183.
(43) Scott, A. P.; Radom, L. *J. Phys. Chem.* **1996**, *100*, 16502.
(44) Andersson, M. P.; Uvdal, P. *J. Phys. Chem. A* **2005**, *109*, 2937.
(45) Blanco, S.; Lesarri, A.; Lopez, J. C.; Alonso, J. L. *J. Am. Chem. Soc.* **2004**, *126*, 11675.
(46) Loh, Z. M.; Wilson, R. L.; Wild, D. A.; Bieske, E. J.; Zehnacker, A. *J. Chem. Phys.* **2003**, *119*, 9559.
(47) Ruoff, R. S.; Klots, T. D.; Emilsson, T.; Gutowsky, H. S. *J. Chem. Phys.* **1990**, *93*, 3142.
(48) Florio, G. M.; Christie, R. A.; Jordan, K. D.; Zwier, T. S. *J. Am. Chem. Soc.* **2002**, *124*, 10236.
(49) Florio, G. M.; Zwier, T. S. *J. Phys. Chem. A* **2003**, *107*, 974.
(50) Godfrey, P. D.; Brown, R. D. *J. Am. Chem. Soc.* **1998**, *120*, 10724.
(51) Godfrey, P. D.; Rodgers, F. M.; Brown, R. D. *J. Am. Chem. Soc.* **1997**, *119*, 2232.
(52) Petrie, S. *Int. J. Mass Spectrom.* **2006**, *255*, 213.
(53) Farnik, M.; Steinbach, C.; Weimann, M.; Buck, U.; Borho, N.; Suhm, M. A. *Phys. Chem. Chem. Phys.* **2004**, *6*, 4614.
(54) Sulkes, M.; Jouvet, C.; Rice, S. A. *Chem. Phys. Lett.* **1982**, *87*, 515.

JP711546P